GENERALIZED TRANSIENT LEVEQUE PROBLEM

Ondrej WEIN

Institute of Chemical Process Fundamentals, Academy of Sciences of the Czech Republic, 165 02 Prague 6-Suchdol, Czech Republic; e-mail: webox@icpf.cas.cz

Received January 24, 1996
Accepted May 20, 1996

Response of an electrodiffusion friction sensor to a finite step of the wall shear rate is studied by numerically solving the relevant mass-transfer problem. The resulting numerical data on transient currents are treated further to provide reasonably accurate analytical representations. Existing approximations to the general response operator are checked by using the obtained exact solution.
Key words: Unsteady mass transfer; Concentration boundary layer; Limiting diffusion current.

In the chemical engineering design[1,2], there is no need for extremely accurate predictions of heat/mass-transfer rates. Commonly, an uncertainty within ±10% seems to be quite acceptable. Such circumstances do not encourage a proper treatment of related mathematical problems. The history of the transient Leveque problem[3,4] can serve as a typical example. The authors[3,4] who analytically solved this rather difficult transient problem in terms of the temperature field and the corresponding local wall fluxes, did not try to convert their solution into the terms of the transient total fluxes, the only measurable quantity[5]. Later attempts[6,7] are even worse in this respect, as they ignore the former exact analyses[3–5].

Fortunately for the mathematics of diffusion, there are fields of pragmatic interest where a rigorous and accurate theoretical prediction of the mass-transfer rates is highly appreciated. One of such fields is related to the scientific instrumentation based on measuring the electrolytic currents under limiting diffusion conditions. With no special device, the current can be determined with an accuracy to 3–4 valid decimal digits. According to the Faraday law, the electrolytic current density is related stoichiometrically to the diffusion fluxes of the species taking part in the electrode reaction[8], $O + e \leftrightarrow R$. Typical applications of such electrolytic cells can be found both in electroanalytical chemistry[8,9] and electrodiffusion (ED) flow measurements[10–13].

There are two important tasks for mathematics of unsteady convective diffusion in the field of ED flow measurements. First, properly evaluated transient experiments provide a powerful tool for the calibration and checking of ED probes during flow measurements[5,12,14,15]. Second, the ED measurements taken under unsteady flow conditions should be corrected for the diffusion inertia of the ED probe. Until now, the only mas-

tered field of the ED inertia effects are harmonically fluctuating flows with a small amplitude of fluctuations[10–13,16]. Transient processes, e.g. response of the ED probe to a passing single particle or turbulent eddy, have not been studied yet at all. It is the purpose of the present paper to analyse the simplest case of transient response related to a finite step of wall shear rate.

THEORETICAL

The essential part of the ED friction probe[10–12] is a working electrode mounted flush with an insulating wall. We consider the rectangular working electrode of a small length $x = L$ and larger width w, see Fig. 1. The electrode is surrounded by a stream of the electrolyte solution containing a depolarizer of a given bulk concentration c^b,

$$c = c^b ; \quad \text{for } z = \infty \ . \tag{1a}$$

The output signal of the ED probe is the electric current $i = i(t)$ but there are at least two operating parameters on the input of this electrochemical system: total overpotential, $U = U(t)$, and the wall shear rate $q = q(t)$.

If both the ohmic and faradaic (kinetic) resistances are negligible in comparison with the transport resistance of the diffusion layer, U is equal to the concentration overpotential[8]. The total overpotential then governs the wall concentration c^w of the depolarizer according to the Nernst equation[8]. Because of a large number of side effects which result in a varying activity of the solid electrode, however, there are only two states of the ED electrolytic cell which can be adjusted with a reasonable accuracy: the *equilibrium* (no-current) state, $U = 0$, with the surface concentration same as in the

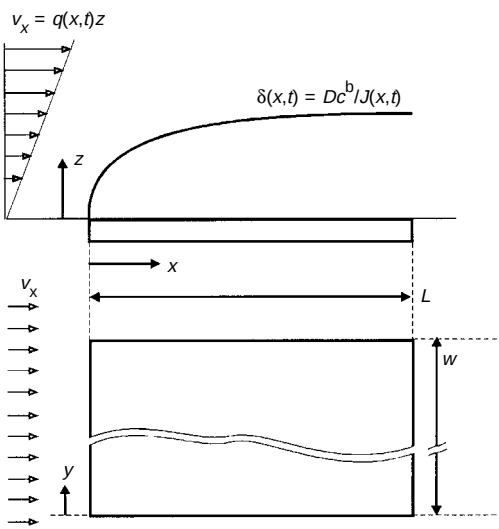

FIG. 1
Rectangular (strip) electrodiffusion friction probe

bulk, $c^w = c^b$, and the *limiting diffusion current* state $|UF/RT| >> 1$, with the zero surface concentration, $c^w = 0$. For a suitable redox couple (e.g. ferro- and ferricyanides) with the same bulk concentration of both forms, the limiting-current state is achieved at total overpotential of 0.7 ÷ 1 V. The only reasonable transient potentiodynamic experiment with ED probes is the step change of overpotential from zero to a value high enough to achieve the limiting diffusion regime,

$$c^w(t) = \begin{cases} c^b; & \text{for } t < 0 \\ 0; & \text{for } t > 0 \end{cases} . \qquad (2)$$

The response of the ED probe under steady flow conditions to this potential step is the subject of classical transient Lévêque problem[3–5] at constant wall shear rate $q(t) = q_s$.

In the present work, we study another transient problem, the response to a finite step change of the wall shear rates

$$q(t) = \begin{cases} q_0; & \text{for } t < 0 \\ q_s; & \text{for } t > 0 \end{cases} , \qquad (3)$$

under limiting diffusion conditions, $c^w(t) = 0$, i.e.

$$c = 0; \quad \text{for } z = 0 . \qquad (1b)$$

The classical transient Leveque problem can be taken as a special case of this problem for an infinite initial wall shear rate, $q_0 = \infty$. Therefore, the transient problem studied in the present paper is more general than the classical one and includes it as a special case.

Under the conditions typical of ED experiments[17], the general transport equation of convective diffusion for the concentration field $c = c(z,t,x)$ of the depolarizer can be simplified, by neglecting the spatial diffusion[18–20] and curvature of the velocity profile, to the form

$$\partial_t c = D\, \partial_{zz} c - q(t) z\, \partial_x c . \qquad (4)$$

The primary response is the limiting diffusion current $i = i(t)$ through the ED probe which can be related to the mean diffusion flux, $\bar{J}$, of the depolarizer,

$$i/F = wx\bar{J}(t,x) \equiv w \int_0^x J(t,x')\, \mathrm{d}x' , \qquad (5)$$

where

$$J(t,x) = D\, \partial_z c(z,t,x)|_{z=0} \qquad (6)$$

is the local diffusion flux. The ultimate aim of solving the transient problem is to determine the mean diffusion flux, $\bar{J} = \bar{J}(t,x)$, according to Eqs (*5*) and (*6*).

Singular Solution and the Convective-Diffusion Wave

There are two well-known simple solutions to the transport equation (*4*) which satisfy the boundary conditions (*1a,b*) and (*2*) of the classical transient Leveque problem[3–5]. The *Leveque*[21] (steady) asymptote gives the steady-state solution for a constant wall shear rate $q = q_s$:

$$C = C_L(\eta(z,x)) \ , \quad J = J_L(x) \ , \quad \bar{J} = \bar{J}_L(x) \ . \tag{7a,b,c}$$

The *Cottrell*[22] (penetration) asymptote characterizes the response of an ED probe in a quiescent liquid, $q = 0$, to the potentiostatic step from equilibrium to limiting diffusion current regime, as described by Eq. (*2*):

$$C = C_C(\zeta(z,t)) \ , \quad \bar{J} = J = J_C(t) \ . \tag{8a,b,c}$$

Notice that the functions $C_L(\eta)$, $J_L(x)$, $\bar{J}_L(x)$, related to the Leveque asymptote, and $C_C(\zeta)$, $J_C(t)$, $\bar{J}_C(t)$, related to the Cottrell asymptote, are defined in the Symbols and Definitions. Using these two asymptotes, it is possible to set up a complete continuous and piecewise continuously differentiable solution to the classical transient Leveque problem[5]. The concentration field

$$C = \mathrm{Max}\{C_C(z,t), C_L(z,x)\} \tag{9}$$

is split into two subdomains, separated by a moving boundary, the convective-diffusion wave (CDW). Kinematics of the CDW can be determined[5] by solving the equation

$$C_C(z,t) = C_L(z,x) \ . \tag{10}$$

In particular, the CDW close to the wall, $z \to 0$, separates the corresponding branches of the local wall fluxes,

$$J(t,x)/J_L(x) = \begin{cases} \theta^{-1/2} ; & \text{for } \theta < 1 \\ 1 ; & \text{for } \theta > 1 \end{cases} \ . \tag{11}$$

The constraint $\theta = 1$, i.e. x is proportional to $D^{1/2}t^{3/2}q_s$, characterizes the movement of the CDW close to the wall. The movement of the CDW in a deep bulk, $z \to \infty$, i.e. outside the concentration boundary layer, $\zeta >> 1$, $\eta >> 1$, can be determined by solving Eq. (*10*) in the corresponding approximation, $\exp(-\eta^3) \approx \exp(-\zeta^2)$. By recalling the definition of θ, the constraint $\eta^3 = \zeta^2$ can be written in the form $\eta\theta = \kappa$ which characterizes the movement of the CDW outside the concentration boundary layer.

For a strip ED sensor of length $x = L$, the transient mean flux calculated from Eq. (*11*) according to definition (*5*) is given by:

$$\bar{J}(t,x)/\bar{J}_{\mathrm{L}}(x) = \begin{cases} \frac{2}{3}\theta^{-1/2} + \frac{1}{3}\theta\ ; & \text{for } \theta < 1 \\ 1 \quad\ ; & \text{for } \theta > 1 \end{cases} . \qquad (12)$$

This approximation to the exact smooth solution[3–5] is commonly used in electrodiffusion applications[14,15].

Similarity Transformation

The original parabolic problem, see partial differential equation (*4*), is three-dimensional, with two "parabolic" variables x and t, and the "diffusion" coordinate z. The boundary conditions in the bulk of streaming solution, $z \to \infty$ and at the electrode surface, $z = 0$,

$$C = 1 \ ; \ \text{for } (x < 0) \text{ or } (z \to \infty) , \qquad (13a,b)$$

$$C = 0 \ ; \ \text{for } (x > 0) \text{ and } (z = 0) , \qquad (13c)$$

are accompanied by the initial condition

$$C = C_{\mathrm{L}}(R\eta) \ ; \ \text{for } (x > 0) \text{ and } (z > 0) \text{ and } (t \le 0) , \qquad (13d)$$

which follows in an obvious way from conditions (*3*) and the Leveque steady-state solution (*7*), applied to $q(t) = R^3 q_{\mathrm{s}}$. The similarity transformation,

$$C = C_{\mathrm{L}}(\eta) + \exp(-\frac{1}{2}\eta^3)\, H(\eta,\theta) , \qquad (14)$$

where H represents the transient deviation from the ultimate steady-state concentration field, reduces this 3D problem to a 2D one,

$$k\,\partial_\theta H = \partial^2_{\eta\eta} H + (3\eta + \frac{9}{4}\eta^4) H , \qquad (15)$$

with the corresponding initial ($\theta = 0$), boundary ($\eta = 0$, $\eta = \infty$), and ultimate ($\theta = \infty$) conditions:

$$H = \exp(\frac{1}{2}\eta^3) \int_{\eta}^{R\eta} \exp(-s^3)\, \mathrm{d}s/\Gamma\left(\frac{4}{3}\right) \ ; \ \text{for } \theta \le 0 , \qquad (16)$$

$$H = 0 \ ; \ \text{for } \eta = 0 \text{ or } \eta = \infty \text{ or } \theta = \infty . \qquad (17a,b,c)$$

The resulting local and mean diffusion fluxes are calculated from the concentration field:

$$\bar{J}(t,x)/\bar{J}_{\mathrm{L}}(x) \equiv M(\theta) = \theta\int_{\theta}^{\infty} N(s)s^{-2}\,\mathrm{d}s \ , \qquad (18)$$

where

$$N(\theta) \equiv \partial_{\eta} H(\eta,\theta)|_{\eta=0} \ . \qquad (19)$$

For reasonable changes of the wall shear rate, say $R < 100$, the response can be represented better in the form

$$L(\theta,R) = (M(\theta) - 1)/(R - 1) \ , \qquad (20)$$

which corresponds to a renormalized problem for the field $H(\theta,\eta)/(R - 1)$. For very small changes of the wall shear rate, $R \to 1$, the problem becomes R-independent, with a parameter-free initial condition,

$$H(\eta)/(R - 1) = \eta \exp\left(-\frac{1}{2}\eta^3\right)/\Gamma\left(\frac{4}{3}\right) ; \quad \text{for } \theta \le 0 \ . \qquad (21)$$

The governing partial differential equation (*15*) displays a feature uncommon in convective diffusion problems: if the term $\partial_{\theta}H$ is always negative, the sign of the parabolic term, $k\,\partial_{\theta}H$, changes across a critical line $\theta\eta = \frac{4}{6}\kappa$ in the domain (θ,η). We note that this singular line corresponds to the CDW which we have observed as a feature typical of the singular solution. Now it becomes evident that the CDW is not merely an artefact of the singular approximation but an actual feature for the class of problems under consideration. The only difference is that the exact solution will display this feature in a slightly smoother form: instead of a shock wave of zero thickness we could expect a thin transient region which separates two subdomains – inner zone of the transient concentration boundary layer with convection and diffusion of comparable importance and the outer zone of the bulk solution where the concentration information from the forward edge of the electrode is spread by convection with the local velocity $q_s z$. It should be noted that this transient substructure has nothing in common with the classical steady concentration boundary layer, which is roughly bounded by the conditions $\eta < 3/R$ for $\theta < 0$ and $\eta < 3$ for $\theta \to \infty$.

Numerical Solution

We intended to solve the parabolic boundary-value problem, Eqs (*15*) and (*16*), and (*17a,b,c*), by the Crank–Nicolson method. Because of the CDW phenomenon, the problem should be considered as a couple of two simultaneous parabolic transient problems,

for the inner ($k > 0$) and outer ($k < 0$) regions with the initial conditions placed in $\theta = 0$ and $\theta = \infty$, respectively. The corresponding partial concentration fields must be matched across the CDW line, $k = 0$. Preliminary numerical experiments have shown two useful facts:

a) Boundary values of the transient concentrations, $H(\eta,\theta)|_{CDW}$, are very low in comparison with the maximum values of H within the inner region.

b) The desired data about the local and mean fluxes are insensitive to the conditions stated in the CDW line, $k = 0$.

In particular, we found two approximate solutions to the given problem which deals only with the inner transient region $\eta < \eta_{CDW}(\theta)$. An additional boundary condition was stated at the CDW line. We tested two variants, using either the *zero estimate*

$$H = 0 \;\; ; \;\; \text{for } \eta = \eta_{CDW}(\theta) \;\; , \tag{22a}$$

or the extrapolation

$$\partial_\eta H = -(\frac{3}{2}\eta - \eta^{-1})H \;\; ; \;\; \text{for } \eta = \eta_{CDW}(\theta) \;\; . \tag{22b}$$

The reason for the first variant is obvious, the second one is motivated by the asymptotic form of the initial condition (*21*) for $R \to 1$, $H \approx \eta \exp(-\frac{1}{2}\eta^3)$. The approximations obtained in this way are compared in Fig. 2 with the final results obtained by the matching method. The following conclusions were drawn from this comparison:

a) The extrapolation, Eq. (*22b*), gives a rough approximation with deviations about 0.3% of $M(\theta)$ from the results of the matching method.

b) The zero estimate, Eq. (*22a*), gives the resulting $M(\theta)$ which coincides with the result of matching method within 0.001%, i.e. to 4–5 valid decimal digits.

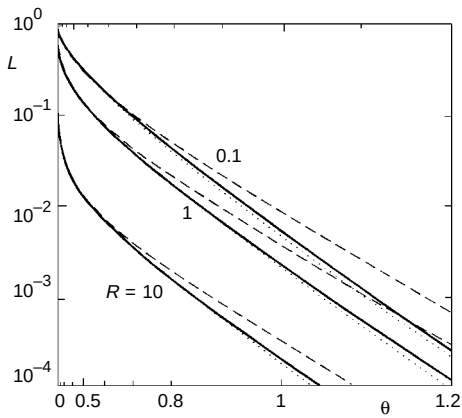

FIG. 2
Effect of approximate estimates of the boundary conditions in the CDW line on the accuracy of resulting transient currents for various R. The trailing parts of the transient curves are linear in the chosen coordinates log (L) – θ^3. Solid lines – exact courses (by the matching method), dotted lines – zero estimate, Eq. (*22a*), dashed lines – extrapolation, Eq. (*22b*)

c) By the matching method, $M(\theta)$ is calculated within the accuracy of 5 valid decimal digits. This conclusion is supported by the comparison of numerical solutions for $R >> 1$ with the exact analytical solution for $R = \infty$.

In the final computations, we have used the zero estimate (*22a*) as a first guess, and the final results were obtained by iteration where the forward computation, $\Delta\theta > 0$, over the inner region alternates with the backward computation, $\Delta\theta < 0$, over the outer region. The partial concentration fields were matched across the CDW line by sharing the neighbouring mesh points from the both subdomains, as shown in Fig. 3. The resulting normalized concentration field $H(\eta,\theta)$ is shown in Fig. 4 for the cases of very high and very low R value. The form of the concentration field obtained by numerical computations suggests a weak singularity, with continuous field but infinitely large gradients at the CDW line.

By choosing a constant-step mesh for the discrete representation of the field $H(\eta,\theta)$,

$$H_j^i = H(\eta_j,\theta^i)\ ;\ \eta_j = j\Delta\eta\ ,\ \theta^i = i\Delta\theta\ , \qquad (23a,b,c)$$

the partial differential equation (*15*) is converted to the difference equations for the forward computations,

$$H_j^i := [(b - a - 1)H_j^{i-1} + \frac{1}{2}(H_{j+1}^i + H_{j+1}^{i-1} + H_{j-1}^i + H_{j-1}^{i-1})]/[b + a + 1]\ ;\ \ b > 0\ , \qquad (24a)$$

with $j = [1..n - 1]$, and for the backward computations,

$$H_j^{i-1} := [(-b - a - 1)H_j^i + \frac{1}{2}(H_{j+1}^i + H_{j+1}^{i-1} + H_{j-1}^i + H_{j-1}^{i-1})]/[-b + a + 1]\ ;\ \ b < 0\ , \qquad (24b)$$

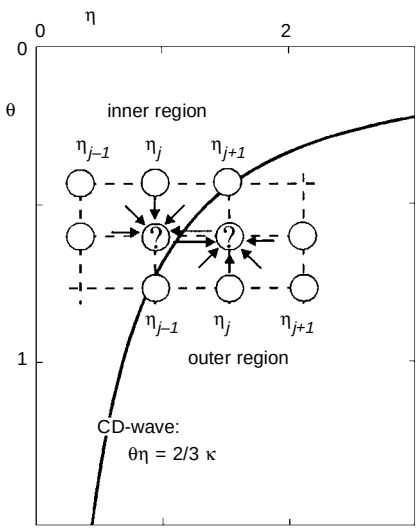

FIG. 3
Crank–Nicolson (6-point cell) method with matching between inner and outer region. In the inner region, the calculation starts at the line $\theta = 0$ with a known non-zero concentration profile, assuming the mesh values H_j^i in the outer region to be known. In the outer region, the calculation starts with the zero concentration profile for $\theta = \theta_{max}$, assuming the mesh values H_j^i in the inner region to be known

with $j = [n..\eta_{max}/\Delta\eta]$. Here,

$$a = \frac{1}{2}(\Delta\eta)^2(3\eta_j + \frac{9}{4}\eta_j^4) \ , \quad b = \frac{(\Delta\eta)^2}{\Delta\theta}(4\kappa - 6\eta_j\theta^{i-1/2}) \ , \qquad (25a,b)$$

and $j = n$ represents the local divide between the inner and outer subdomains,

$$\eta_{n-1} < \eta_{CDW}(\theta) \le \eta_n \ . \qquad (26)$$

The system of linear difference equations, with the zero boundary conditions $H = 0$ located at the edges $\eta = 0$ and $\eta = \eta_{max}$, is solved in an iterative way for the mesh values H_j^i stabilized to 7 decimal digits.

The wall fluxes are calculated, assuming $H \approx k_1\eta + k_2\eta^4$ for $\eta \to 0$, from the formula

$$N^i = N(\theta^i) = (16H_1^i - H_2^i)/14\Delta\eta \ , \qquad (27)$$

and then integrated according to the definition (*18*) for non-zero $\theta^{i-1} = \theta^i - \Delta\theta$, by the modified trapezoidal rule,

$$\int_{\theta^{i-1}}^{\theta^i} N(s)s^{-2}\,\mathrm{d}s = N^{i-1}\left[\frac{1}{\theta^{i-1}} - \frac{1}{\Delta\theta}\ln\frac{\theta^i}{\theta^{i-1}}\right] + N^i\left[\frac{1}{\Delta\theta}\ln\frac{\theta^i}{\theta^{i-1}} - \frac{1}{\theta^i}\right] , \qquad (28)$$

which reflects the singularity for $N(\theta) = \text{const}$ at very low θ.

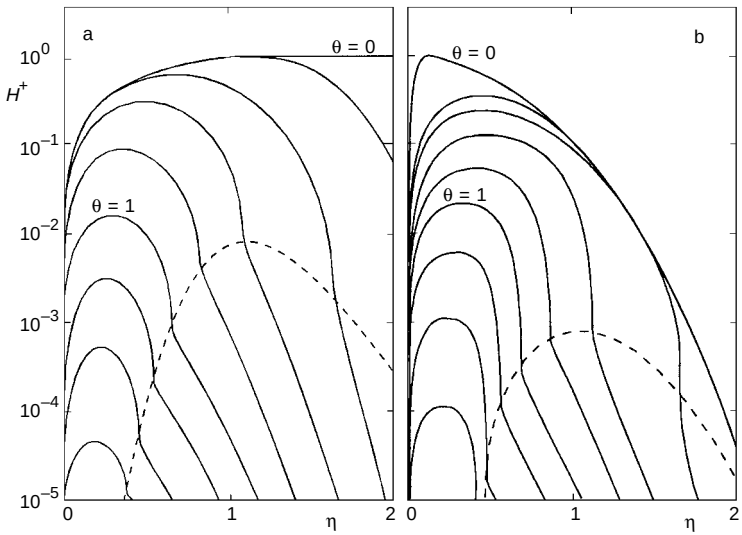

FIG. 4

Normalized concentration profiles, $H^+ = H(\eta,\theta)/H_{max}$, for $R = 0.1$ (a) and $R = 10$ (b). The profiles are given for θ ranging from 0 to 1.6 with constant step $\Delta\theta = 0.2$. The dashed lines correspond to the CDW line which separates inner and outer region

RESULTS

Accuracy of Computations, Way of Presenting the Results

Strictly speaking, we got only an approximate numerical solution without a firm estimate of its accuracy. The extent of errors due to a finite-size discrete mesh was checked by modifying the step lengths $\Delta\theta$ and $\Delta\eta$ as well as the actually covered domain $\theta \in (0;\theta_{max})$, $\eta \in (0,\eta_{max})$. We found that the steps $\Delta\theta = 5 \cdot 10^{-5}$, $\Delta\eta = 1 \cdot 10^{-2}$, and the actual boundaries of the unlimited domain, $\theta_{max} = 4$, $\eta_{max} = 3$, guarantee the mean flux data $M = M(\theta)$ stable to 5 decimal digits. The forward/backward matching iterative process was terminated after stabilizing the mean flux data to the same level of accuracy. Therefore, we estimate the final accuracy of all the obtained data on the mean fluxes $M = M(\theta)$ to 5 valid decimal digits.

For a given R, the primary results are given by a set of discrete values of the function $M = M(\theta)$ or $L = L(\theta)$ over the interval $\theta \in [0..\theta_{max}]$ with the step $\Delta\theta = 1 \cdot 10^{-2}$. These discrete data were condensed, using non-linear least-squares fitting, to suitable empirical formulas with accuracy better than 0.03% (4÷5 valid decimal digits) of the current value of M. The computed mean transient fluxes for the full range of parameter R are shown in Fig. 5 for several values of R.

Classical Transient Leveque Problem, $R \to \infty$

The classical transient Leveque problem differs from the generalized one (stated in the former paragraphs) by a slightly different initial condition, see Eq. (*2*), which corresponds to a step change of the wall shear rate from an infinitely large value to a finite one, q_s. The classical transient problem can be solved analytically to provide the local flux densities[4] in the form of an infinite series

$$N(\theta) = 1 + 3^{1/3}\Gamma\left(\frac{1}{3}\right)\sum_{n=1}^{\infty} a_n^{-1} \exp\left(-\frac{2}{3}\vartheta_n^3\right) \mathrm{Ai}(\vartheta_n^2) \ , \qquad (29)$$

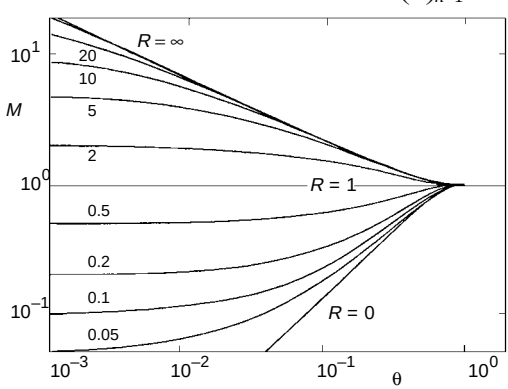

FIG. 5
Normalized mean transient currents for the complete R-domain

where $-a_n < 0$ stand for the zeroes of the Airy function, $\mathrm{Ai}(-a_n) = 0$, and

$$\vartheta_n = a_n t D^{1/3} (3x/q_s)^{-2/3} = 3^{2/3} a_n \theta/(4\kappa) \quad . \tag{30}$$

We do not know how to integrate the series (*29*) analytically. Within accuracy of 5 valid decimal digits, the result of numerical integration of the function $N(\theta)$ was expressed by the semiempirical formula[5]

$$M(\theta) = \begin{cases} (\frac{9}{4}\theta)^{-1/2} + \frac{102}{300}\theta - \frac{3}{800}\theta^{11} ; & \text{for } \theta < 1 \\ 1 + \frac{43}{520} \exp(-\frac{10}{3}\theta^3) ; & \text{for } \theta > 1 \end{cases} . \tag{31}$$

Noticeably, the maximum relative deviation of the exact result (*31*) from the rather trivial singular solution (*12*) does not exceed 0.53%.

Start-Up Flow Case, $R \to 0$

The case $R = 0$ is related to no-flow state prior to the start of the experiment, $t = 0$. There is no physically reasonable steady-state solution to the problem of two-dimensional diffusion in a quiescent solution (by analogy with the diffusion to a cylinder in an infinite volume). However, the corresponding transient problem for the initial conditions

$$H = -\exp(\tfrac{1}{2}\eta^3) \int_0^\eta \exp(-s^3)\, \mathrm{d}s/\Gamma\left(\frac{4}{3}\right) ; \quad \text{for } \theta = 0 \ , \tag{32}$$

seems to be a well-posed one, with a unique regular solution. Noticeably, the same boundary-value problem corresponds to another hypothetical physical situation, with the solution quite depleted of the active component, $c = 0$, prior to the start, $t < 0$, and then replaced by the fresh solution in the half space $x < 0$ just at the starting moment, $t = 0$. In practice, this asymptotical problem is related to cases of very slow flow prior to the step change, $q_0 << q_s$. By treating the numerical data, we obtained the following empirical representation of $M(\theta)$,

$$M(\theta) = \begin{cases} 1.405245\theta & ; \ \theta < 0.3 \\ 1 - \exp(-4\theta^3)(0.8948 - 0.8613\theta + 0.2530\theta^2) & ; \ \theta > 0.3 \end{cases} . \tag{33}$$

Linear Approximation, $R \to 1$

The linearization consists in solving the problem for very small changes of the wall shear rates, i.e. for $R \to 1$. The problem of determining $L_1(\theta) \equiv L(\theta; R = 1)$ provides no simplification of the general boundary-value problem under consideration. It only changes the initial condition (*16*) to the form (*21*) which contains no parameter. By fitting the numerical results for $|R - 1| < 10^{-2}$, we obtained the following representation,

$$L_1(\theta) = \begin{cases} 1 - 4.0979\theta + 3.4832\theta^{3/2} - 0.3830\theta^3 & ;\ \theta < 0.9 \\ \exp(-4\theta^3)(0.654 - 1.0276\theta + 0.4921\theta^2) & ;\ \theta > 0.9 \end{cases}, \qquad (34)$$

with the accuracy of 5 valid digits, or

$$L_1(\theta) = \begin{cases} (1 - \theta/1.5)^5 & ;\ \theta/1.5 < 1 \\ 0 & ;\ \theta/1.5 > 1 \end{cases}, \qquad (35)$$

with the accuracy of 3–4 valid digits.

Retarded, R > 1.1, and Accelerated, R < 0.9, Flows

Retarded flows correspond to a step decrease of the wall shear rate, i.e. $R < 1$, and accelerated flows to a step increase, i.e. $R > 1$. The correlation of the numerically simulated data on $M = M(\theta;R)$ does not include the interval $R \in (0.9;1.1)$ which is fitted within the frame of linear dynamics approximation, see Eqs (*34*), (*35*). The following correlations fit a function of two independent arguments. Rather rough approximations were accepted, with accuracy to 3–4 valid decimal digits, for the sake of simplicity of the empirical formulas. For retarded flows, $R > 1.1$:

$$M(\theta) = \begin{cases} \left[(R^{-2} + \frac{9}{4}\theta)^{1/2} - (0.0028 + 1.0488R^{-2})\theta - (0.7628 - 0.8662R^{-2})\theta^2 + 0.25\theta^3\right]^{-1} & ;\ \theta < 0.6 \\ 1 + \exp\left[(1.0938 - 0.1615R^{-1})\theta^3\right](0.062R^{-2} - 0.0508)(\theta^{-1} - 1.1297\theta^{-2}) & ;\ \theta > 0.6 \end{cases}. \qquad (36)$$

For accelerated flows, $R < 0.9$, with $r = 1 - R > 0$:

$$M(\theta) = \begin{cases} R + (1.3904(1 - R^2) + 0.0838R)\theta - (1.3773R - 1.1233R^2 + 2.487R^3)\theta^2 & ;\ \theta < 0.3 \\ 1 - \dfrac{\exp\left[-(3.7 + 0.222r + 0.200r^2)\theta^3\right]}{0.148 + 1.020r^{-1} + [2.196r^{-1} + 1.829r^{-2} - 1.709]\theta^{3/2}} & ;\ \theta > 0.3 \end{cases}. \qquad (37)$$

DISCUSSION

The ED friction probes operating under limiting diffusion conditions can be understood as a non-linear dynamic system with a single input $q = q(t)$ and a single output $i = i(t)$ or $\bar{J} = \bar{J}(t)$, see Eq. (*5*). The dynamic calibration should result in a complete knowledge of the response operator $\Re$,

$$\bar{J}(t) = \Re\{q(t)\}, \qquad (38)$$

for any admissible history of the wall shear rates, $q = q(t)$. In reality, representations of this non-linear operator are known only for a very limited class of the flow histories:

a) Linear approximation[10–12] for superposed harmonic fluctuations of q with small amplitude. Large-amplitude superposed harmonic fluctuations were also studied[25] by

numerical solving the partial differential equation (*4*). Unfortunately, these results were not represented in an analytic form, suitable for data treating and hence they are not discussed here.

b) Semiempirical[5,12,23] and local-similarity[24] approximation for slow changes of q.

It is the purpose of the remaining paragraphs to confront these two analytical approximations with the presented results.

Relation to Linear Dynamics for Small Fluctuations

To apply the well-known procedures of linear dynamics to a non-linear response operator, some systematic approximation scheme must be introduced. Let us consider a flow history in the form

$$q(t) - q_s = q_s\, \varepsilon(t) \ , \tag{39}$$

assuming the relative amplitude of the fluctuations, $\varepsilon_0 \equiv \mathrm{Max}\{|\varepsilon(t)|\}$, to be very small. The response operator, neglecting the second-order effects, $O(\varepsilon_0)^2$, can be linearized to the form

$$\bar{J}(t) - \bar{J}_s = \bar{J}_s \int_{-\infty}^{t} K(t-s)\, \mathrm{d}\varepsilon(s) \ . \tag{40}$$

Here, $\bar{J}_s = \bar{J}_L(x)$ is the steady-state mean diffusion flux for $q(t) = q_s$. The kernel $K(t)$ in the Lebesgue convolution integral (*40*) is the response of the linear system to a step change of the input signal:

$$\bar{J}(t) - \bar{J}_s = \bar{J}_s \varepsilon_0 K(t) \ ; \quad \text{for} \ \ q(t) - q_s = q_s \varepsilon_0 \Upsilon(t) \ . \tag{41}$$

Here, $\Upsilon(t)$ stands for the Heaviside unit step function.

We have studied the linear response operator in a slightly different way, but it is an easy task to prove the identity

$$K(t) = \frac{1}{3}[1 - L_1(t/t_s)] \ . \tag{42}$$

The limits of applicability of the linearized representation follow from the test shown in Fig. 6. For $|R - 1| < 0.1$, i.e. for $\varepsilon_0 < 0.3$, the deviations of the exact (non-linear) responses to the step change in q from the linearized one are smaller than 10% of the actual value of $(\bar{J}(t) - \bar{J}_s)$.

A simple approximate representation of $K(t)$ follows from Eq. (*35*):

$$K(t) = \begin{cases} 0 & ; \quad t < 0 \\ \frac{1}{3}(1 - (1 - t/t_1)^5) & ; \quad 0 < t < t_1 \\ \frac{1}{3} & ; \quad t_1 < t \end{cases} , \tag{43}$$

with $t_1 = 1.5\ t_s = 1.648 x^{2/3} q_s^{-2/3} D^{-1/3}$. The corresponding linearized response operator for a general small-amplitude flow history can now be written in the simple form

$$\bar{J}(t)/\bar{J}_s - 1 = \frac{1}{3}[1 - \int_{t-t_1}^{t} (1 - \frac{t-s}{t_1})^5 \, \mathrm{d}\varepsilon(s)] \ . \tag{44}$$

The response to small-amplitude superposed harmonic fluctuations, $\varepsilon(t) = \varepsilon_0 \exp(\mathrm{i}\omega t)$, is given by $\bar{J}(t)/\bar{J}_s - 1 = \varepsilon_0 K^*(\omega) \exp(\mathrm{i}\omega t)$, where the complex impedance K^*,

$$K^*(\omega) \equiv K(\infty) + \mathrm{i}\omega \int_0^\infty [K(s) - K(\infty) \exp(-\mathrm{i}\omega s) \, \mathrm{d}s \ , \tag{45}$$

can be expressed from the approximation (*43*) in the closed form:

$$K^*(\omega) = \frac{1}{3}[1 - \mathrm{i}p \exp(-\mathrm{i}p) \int_0^1 s^N \exp(\mathrm{i}ps) \, \mathrm{d}s] = \frac{1}{3} \sum_{k=0}^{\infty} \frac{N!}{(k+N)!} (-\mathrm{i}p)^k \ , \tag{46}$$

where $N = 5$ and

$$p = \omega t_1 = 1.648 \omega x^{2/3} q_s^{-2/3} D^{-1/3} \ . \tag{47}$$

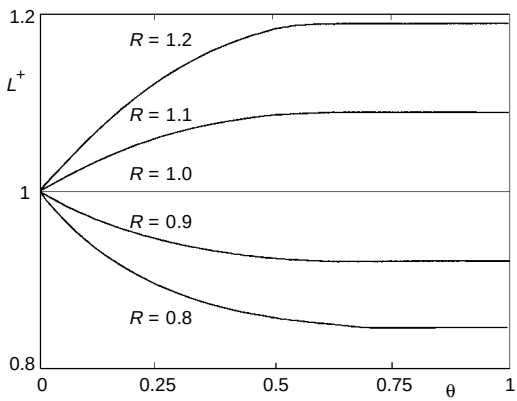

FIG. 6
Limits of the linearization for finite values of $(R - 1)$. The relative errors are expressed as deviation of $L^+(\theta) = L(\theta,R)/L_1(\theta)$ from unity

The corresponding phase shift

$$\Phi = \arctan\left(\mathrm{Im}\{K^*(\omega)\}/\mathrm{Re}\{K^*(\omega)\}\right) \qquad (48a)$$

and amplitude ratio

$$A = |K^*(\omega)/K^*(0)| \qquad (48b)$$

are compared in Fig. 7 with the results[13] of direct exact calculations.

Relation of the Slow-Motion Asymptote to Similarity Approximation

In ED practice, the most common approximation to the non-linear response operator is the quasi-steady asymptote,

$$\bar{J}(t) = \beta_L q^{1/3}(t) \ , \quad \beta_L = D^{2/3} c^b / (2\Gamma(\frac{4}{3}) x^{1/3}) \qquad (49a,b)$$

which tacitly assumes immediate response of the probe to any change of wall shear rates. Assuming a similarity concentration profile in the concentration boundary layer, the simple non-linear model[5,7,12,23]

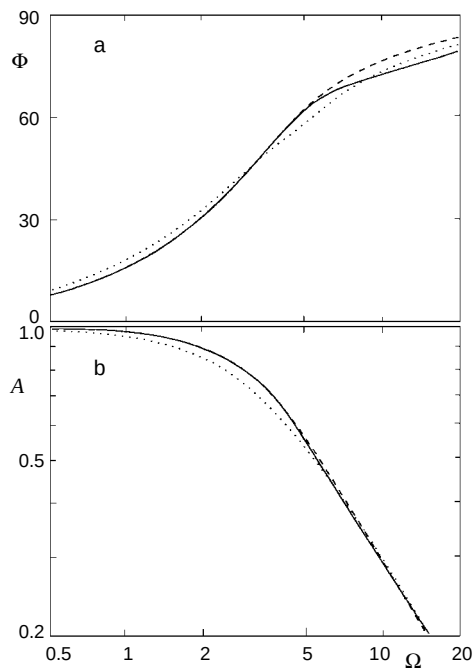

FIG. 7
Various ways of calculating the convective-diffusion impedance of the ED probe. (a) Phase shift Φ (in degrees); (b) reduced amplitude, *A*. Solid lines – exact values[13], dotted lines – global similarity approximation[12], dashed lines – calculated from the linearized response function, Eq. (*46*)

$$q(t) = \beta_L^{-3}\left[\overline{J^3}(t) + \beta_C \frac{d\bar{J}(t)}{dt}\right], \quad \beta_C = 2(c^b)^2 D/\pi \qquad (50a,b)$$

follows directly from the integral form of the transport equation (*4*). The coefficients β_L, β_C are adjustable and can be determined from an appropriate dynamic calibration experiment. Their estimates by (*49b*), (*50b*) are obtained assuming the Leveque and Cottrell asymptotes of the classical Leveque transient process to be the calibration experiments.

The linearized response to the small-amplitude superposed harmonic fluctuations according to this model was studied recently[7,12]. The resulting representation of the impedance, given by the simple formula,

$$K^*(\omega) = 1/(3 + 2i\omega t_0)\,, \quad t_0 = \beta_C/(2\beta_L^2 q_s^{2/3}) = 0.488 x^{2/3} q_s^{-2/3} D^{-1/3} \qquad (51a,b)$$

is compared with the exact linear results in Fig. 7.

CONCLUSION

The non-linear dynamics of the ED friction probes was studied for the finite step change of wall shear rate, a new class of motions not studied till now.

The numerical results were represented by a set of empirical representations with high accuracy (4–5 valid decimal digits) in a form suitable for further computer experiments.

The transient time t_s depends only on the new (steady) value of wall shear rate, q_s. At longer times, $t > t_s$, the remaining perturbation fades out very quickly, proportional to $\exp(-(t/t_s)^3)$, and is quite negligible. This indicates that ED probes display strongly fading memory.

The linearized response operator for a general class of unsteady motion with small fluctuations was approximated by a simple integral, Eq. (*44*), and checked by comparing with the known solution for the harmonic superposed fluctuations.

SYMBOLS AND DEFINITIONS

$c = c(z,x,t)$	concentration field of depolarizer
c^b	bulk concentration
c^w	wall concentration
$C = c/c^b$	normalized concentration
$C_L(\eta) \equiv \int_0^\eta \exp(-s^3)\,ds/\Gamma\left(\frac{4}{3}\right)$	Leveque asymptote for C, Eq. (*7a*)
$C_C(\zeta) \equiv \int_0^\zeta \exp(-s^2)\,ds/\Gamma\left(\frac{3}{2}\right)$	Cottrell asymptote for C, Eq. (*8a*)
D	diffusivity of depolarizer
$\boldsymbol{F}$ = 96484.56 C mol^{-1}	Faraday constant
$H = H(\eta,\theta)$	renormalized transient part of C, see Eq. (*14*)

$H_j^i = H(\eta_j,\theta^i)$ discrete representation to H on constant-step mesh
i electric current
$J(x,t)$ local diffusion flux at point x, Eq. (*6*)
$\bar{J}(x,t)$ mean diffusion flux for electrode of length x, Eq. (*5*)
$J_L(x) = Dc^b/(\Gamma\left(\frac{4}{3}\right)\sigma(x))$ Leveque asymptote to J, Eq. (*7b*)
$\bar{J}_L(x) = \frac{3}{2}J_L(x)$ Leveque asymptote to $\bar{J}$, Eq. (*7c*)
$\bar{J}_C(t) = J_C(t) = Dc^b/(\Gamma\left(\frac{3}{2}\right)\tau(t))$ Cottrell asymptote to J, $\bar{J}$, Eqs (*8b,c*)
$k(\eta,\theta) = (4\kappa - 6\eta\theta)$ variable coefficient at parabolic term, Eq. (*15*)
$L(\theta,R)$ renormalized transient mean flux, Eq. (*20*)
$L_1(\theta) = L(\theta,1)$ asymptote of $L(\theta,R)$ for $R \to 1$, Eqs (*34*), (*35*)
$M(\theta) = \bar{J}(t,x)/\bar{J}_L(x)$ normalized mean flux, Eq. (*18*)
$N(\theta) = J(t,x)/J_L(x)$ normalized local flux, Eq. (*19*)
$q = q(t)$ wall shear rate
q_0 starting value of q, Eq. (*3*)
q_s final (steady) value of q, Eq. (*3*)
$\boldsymbol{R}$ = 8.31434 J K^{-1} mol^{-1} gas constant
$R = (q_0/q_s)^{1/3}$
T thermodynamic temperature
t time
$t_s = 9^{1/3}/4\kappa)D^{-1/3}(x/q_s)^{2/3}$ transient time for electrode of length x
w electrode width, see Fig. 1
x distance to forward edge, see Fig. 1
x electrode length $x = L$, see Fig. 1
z distance to surface, see Fig. 1
$\zeta = z/\tau(t)$
$\eta = z/\sigma(x)$
$\eta_{CDW}(\theta) = \frac{3}{2}\kappa/\theta$ CDW-line between inner and outer region of transient diffusion layer
$\theta = \kappa\tau^2/\sigma^2 = t/t_s$ normalized time
$\kappa = \Gamma^2\left(\frac{3}{2}\right)/\Gamma^2\left(\frac{4}{3}\right) = 0.98493346$
$\sigma(x) = (9Dx/q_s)^{1/3}$
$\tau(t) = (4Dt)^{1/2}$
$\Omega = \omega x^{2/3}D^{-1/3}q_s^{-2/3}$ normalized frequency of flow fluctuations

This work was supported by the Grant Agency of the Academy of Sciences of the Czech Republic under contracts A4072502 and A472312.

REFERENCES

1. Coulson J. M., Richardson J. F.: *Chemical Engineering II.* Pergamon, Oxford 1978.
2. Charpentier J. C.: Adv. Chem. Eng. *11*, 1 (1981).
3. Hudson J. L., Bankoff S. G.: Chem. Eng. Sci. *19*, 591 (1964).
4. Soliman M., Chambre P. L.: Int. J. Heat Mass Transfer *10*, 169 (1967).
5. Wein O.: Collect. Czech. Chem. Commun. *46*, 3209 (1981).

6. Lapicque F., Hornut J. M., Valentin G., Storck A.: J. Appl. Electrochem. *19*, 889 (1989).
7. Wang D. M., Tarbell J. M.: Int. J. Heat Mass Transfer *36*, 4341 (1993).
8. McDonald D. D.: *Transient Techniques in Electrochemistry*. Plenum Press, New York 1977.
9. Stulik K., Pacakova V.: *Electroanalytical Measurements in Flowing Liquids*. Ellis Horwood, Chichester 1987.
10. Hanratty T. J., Campbell J. A. in: *Fluid Mechanics Measurements* (R. J. Goldstein, Ed). Hemisphere Publ. Corp., Washington 1983.
11. Nakoryakov V. E., Burdukov A. P., Kashinski O. N., Geshev P. I.: *Elektrodiffuzionnyi metod issledovaniya lokalnoi struktury turbulentnykh techenii*. Institute of Thermophysics, Novosibirsk 1986.
12. Pokryvaylo N. A., Wein O., Kovalevskaya N.D.: *Elektrodiffuzionnaya diagnostika techenii v suspenziyakh i polimernykh rastvorakh*. Nauka i Tekhnika, Minsk 1988.
13. *Proceedings of the 3rd Workshop on Electrodiffusion Diagnostics of Flow* (C. Deslouis and B. Tribollet, Eds). Dourdan, France 1993.
14. Wein O., Kovalevskaya N. D.: Collect. Czech. Chem. Commun. *49*, 1297 (1984).
15. Sobolik V., Wein O., Wichterle K.: *Proceedings of the 4th Workshop on Electrodiffusion Diagnostics of Flow*, p. 13. Lahnstein, Germany 1996.
16. Deslouis C., Gill O., Tribollet B.: J. Fluid. Mech. *215*, 85 (1990).
17. Wein O.: Collect. Czech. Chem. Commun. *55*, 2404 (1990).
18. Wein O.: Collect. Czech. Chem. Commun. *53*, 1671 (1988).
19. Aoki K., Osteryoung J.: J. Electroanal. Chem. *122*, 19 (1981); errata see: J. Electroanal. Chem. *160*, 335 (1984).
20. Oldham K. B.: J. Electroanal. Chem. *122*, 1 (1981).
21. Leveque M. A.: Ann. Mines, Mem., Ser. 12 *13*, 381 (1928).
22. Cottrell F. G.: Z. Phys. Chem. *42*, 385 (1903).
23. Sobolik V., Wein O., Cermak J.: Collect. Czech. Chem. Commun. *52*, 913 (1987).
24. Wein O.: Ref.[13], p. 3.
25. Mao Z., Hanratty T. J.: Int. J. Heat Mass Transfer *34*, 281 (1991).